Insights into Human Norovirus Cultivation in Human Intestinal Enteroids

Khalil Ettayebi[a], Gurpreet Kaur[a], Ketki Patil[a], Janam Dave[a], B. Vijayalakshmi Ayyar[a], Victoria R Tenge[a], Frederick H. Neill[a], Xi-Lei Zeng[a], Allison L. Speer[b], Sara C. Di Rienzi[a], Robert A. Britton[a], Sarah E. Blutt[a], Sue E. Crawford[a], Sasirekha Ramani[a], Robert L. Atmar[a,c], Mary K. Estes[a,c*]

[a]Department of Molecular Virology and Microbiology, Baylor College of Medicine (BCM), Houston, TX, USA

[b]Department of Pediatric Surgery, McGovern Medical School at the University of Texas Health Science Center at Houston (UTHealth), Houston, TX, USA

[c]Department of Medicine, BCM, Houston, TX, USA

Keywords: HuNoV cultivation, enteroids, organoids, organoid growth media

*Address correspondence to Mary K. Estes, mestes@bcm.edu

Abstract

Human noroviruses (HuNoVs) are a significant cause of epidemic and sporadic acute gastroenteritis worldwide. The lack of a reproducible culture system hindered the study of HuNoV replication and pathogenesis for almost a half-century. This barrier was overcome with our successful cultivation of multiple HuNoV strains in human intestinal enteroids (HIEs), which has significantly advanced HuNoV research. We optimized culture media conditions and generated genetically-modified HIE cultures to enhance HuNoV replication in HIEs. Building upon these achievements, we now present new insights to this culture system, which involve testing different media, unique HIE lines, and additional virus strains. HuNoV infectivity was evaluated and compared in new HIE models, including HIEs generated from different intestinal segments of individual adult organ donors, HIEs from human intestinal organoids produced from directed differentiation of human embryonic stem cells into intestinal organoids that were transplanted and matured in mice before making enteroids (H9tHIEs), genetically-engineered (J4*FUT2* knock-in [*KI*], J2*STAT1* knock-out [*KO*]) HIEs, as well as HIEs derived from a patient with common variable immunodeficiency (CVID) and from infants. Our findings reveal that small intestinal HIEs, but not colonoids, from adults, H9tHIEs, HIEs from a CVID patient, and HIEs from infants support HuNoV replication with segment and strain-specific differences in viral infection. J4*FUT2-KI* HIEs exhibit the highest susceptibility to HuNoV infection, allowing the cultivation of a broader range of GI and GII HuNoV strains than previously reported. Overall, these results contribute to a deeper understanding of HuNoVs and highlight the transformative potential of HIE cultures in HuNoV research.

Importance

HuNoVs cause global diarrheal illness and chronic infections in immunocompromised patients. This manuscript reports approaches for cultivating HuNoVs in secretor positive human intestinal enteroids (HIEs). HuNoV infectivity was compared in new HIE models, including ones from i) different intestinal segments of single donors, ii) human embryonic stem cell-derived organoids transplanted into mice, iii) genetically-modified lines, and iv) a patient with chronic variable immunodeficiency disease. HIEs from small intestine, but not colon, support HuNoV replication with donor, segment and strain-specific variations. Unexpectedly, HIEs from one donor are resistant to GII.3 infection. The genetically-modified J4*FUT2-KI* HIEs enable cultivation of a broad range of GI and GII genotypes. New insights into strain-specific differences in HuNoV replication in HIEs support this platform for advancing understanding of HuNoV biology and developing potential therapeutics.

Introduction

Human noroviruses (HuNoVs) are the most common cause of both epidemic and sporadic acute gastroenteritis worldwide. They also cause chronic infections in immunocompromised cancer, transplant patients, and patients with primary immune deficiencies and are a severe health burden for this population (1-3). Annually, HuNoV infections are responsible for 685 million cases of diarrhea and over 212,000 deaths globally (4). In the United States alone, these infections lead to approximately 109,000 hospitalizations, generating a substantial economic impact of more than $10.6 billion in healthcare expenses and societal costs (4-6). Even though HuNoV was discovered in

1968, there are still no FDA-approved vaccines and efficacious therapeutics available, highlighting the challenges associated with combating these infections and the need for further research and development in this area (7, 8).

One of the main obstacles in studying and understanding HuNoVs was the absence of a culture system to effectively cultivate these viruses. However, in 2016, a significant breakthrough was achieved with the establishment of the human intestinal stem cell-derived enteroid (HIE) system for HuNoV cultivation (9). This development overcame a five-decade barrier in laboratory models for HuNoVs, opening new avenues for investigating HuNoV biology. Since the establishment of the HIE system, significant advancements have been made in unraveling various aspects of HuNoV biology, including strain-specific differences in replication, methods of virus inactivation, innate immune responses, antiviral susceptibility, and characterization of neutralizing antibodies (10-29). Here, we report further advancements in the HIE culture system by testing HuNoV infection in multiple unique HIE lines and expanding the profile of cultivatable HuNoV strains.

Results

We previously reported that differentiation of HIEs and infection carried out in the commercial IntestiCult™ Organoid Growth Medium (OGMd referred to as INTd in (23)) from STEMCELL Technologies (formerly known as IntestiCult media) supports robust replication of HuNoV strains that replicated poorly in HIEs grown in our original in-house culture medium (23). A new IntestiCult™ Organoid Differentiation Medium (ODM) media (also from STEMCELL Technologies) became available in 2020, and we conducted a

comparative analysis between OGM media and the new ODM media to assess their impact on HuNoV replication. For these studies, we used the previously reported genetically-modified J4*FUT2-KI* HIE line in which the fucosyltransferase 2 (*FUT2*) gene was knocked-in to the secretor negative J4 HIE (30). The J4*FUT2-KI* HIE line showed better HuNoV binding to the HIE cell surface and replication of several HuNoVs (30). J4*FUT2-KI* HIE monolayers, seeded in the proliferation OGM medium (OGMp) and then differentiated in either OGMd or ODM media, were infected with a GII.4 Sydney[P31] or a GII.3[P21] HuNoV strain. Both media supported viral replication. However, replication of both strains was enhanced based on significant greater geometric mean $\log_{10}$ genome equivalent (GE) increases in virus yields from 1 hour post infection (hpi) to 24 hpi in HIEs differentiated using OGMd media when compared to ODM media (Figure 1). Consequently, all subsequent experiments described in this study were executed using OGM media. Infections were conducted using the OGMd medium supplemented with the bile acid sodium glycochenodeoxycholate (GCDCA), necessary for GII.3 infection and enhancing GII.4 infection (9).

We next conducted a comparative investigation of viral replication using multiple, unique secretor positive HIE lines derived from various sources. We aimed to capture segment-specific and strain-specific differences in the susceptibility of HIE lines that may influence viral replication. We first evaluated HIEs generated from intestinal tissues obtained from four independent organ donors (designated 2002, 2003, 2004, and 2005). From each donor, four HIE lines were established, representing the three segments of the small intestine [duodenum (D), jejunum (J), and ileum (I)] as well as the colon (C). The HIE lines were confirmed to be secretor positive through genotyping assays for

fucosyltransferase 2 (*FUT2*), which indicated their ability to express the histoblood group antigens (HBGAs) necessary for HuNoV infection. The susceptibility of HIE lines to HuNoV strains GII.4 Sydney[P31] and GII.3[P21] was assessed, focusing on segment-specific differences (Table 1).

GII.4 replication was observed across all small intestinal HIE lines. For GII.4, the yields from the duodenal HIE lines were similar between the lines except 2004 was significantly greater than 2002 ($p<0.01$). For GII.4, the yields in the jejunal HIE lines were similar across all four lines. The yields for GII.4 in the ileal HIE lines were significantly different from each other ($p<0.01$) except between the 2002 and 2003 lines.

GII.3 replication occurred in HIE lines generated from small intestinal segments of three out of the four donors. Unexpectedly, GII.3 replication was not detected in any of the HIEs generated from donor 2003. Comparing replication in the other three lines, GII.3 yield in the duodenal 2004 HIE was significantly greater than in 2002 and 2005 ($p<0.05$) HIEs. In the jejunal lines, GII.3 yield was significantly less in 2005 compared to 2002 ($p<0.01$) and 2004 ($p<0.05$). In the ileal lines, GII.3 yield was significantly less in the 2005 line than in the 2002 ($p<0.001$) and 2004 ($p<0.05$) lines.

None of the colonic HIE lines supported replication of either GII.3 or GII.4 HuNoV strains. These observations suggest that while small intestinal HIE lines are generally permissive to HuNoV infection, there may be variations in viral replication efficiency within different segments of the small intestine from individual donors but data from more HIE lines are needed for definitive conclusions. The observed striking difference in infectivity between GII.4 and GII.3 HuNoV for HIEs from donor 2003 also indicates strain-specific differences in susceptibility to infection within the same donor that are

independent of FUT2 expression. The 2003 line is the first secretor positive HIE line that we have tested that does not support GII.3 replication. Further, these findings confirm our previous report of lack of replication in colonic lines derived from different independent individuals (23), indicating segment-specific differences in the susceptibility of HIE lines to HuNoV infection.

In addition, we assessed HuNoV infection in other unique HIEs. First, we evaluated viral replication in HIEs generated from directed differentiation of H9 human embryonic stem cells (H9hESC) into intestinal organoids (HIOs) that were transplanted and matured in immunocompromised mice for 8 weeks before making enteroids (referred to in this paper as H9tHIEs). The initial HIOs contained both epithelial and mesenchymal cells (31). Previous RNASeq analyses of such HIOs showed these cultures exhibit a more fetal-like transcriptional expression pattern; they are therefore considered immature (32). However, *in vivo* transplantation of such HIOs into mice (tHIOs) induces maturation of the intestinal epithelium resulting in tHIOs with a more adult-like transcriptional profile and enhanced levels of tight junction proteins (32-35). Additionally, the morphology and cellular maturation patterns in tHIOs are similar to fetal intestinal epithelial development (36). For example, an 8-week-old tHIO demonstrates proliferation confined to the crypts similar to a gestational week 18 human fetal intestine (36). To investigate whether matured tHIOs could be susceptible to HuNoV infection, we transplanted immature HIOs under the kidney capsule of immunocompromised mice. After eight weeks, the matured tHIOs were harvested and processed to proliferate into three-dimensional H9tHIEs, following the same protocol used for generating HIEs from human intestinal tissues and biopsies. The resulting H9tHIEs could be passaged

indefinitely, and they also are epithelial only cultures without an outer mesenchyme, a morphology similar to tissue stem cell-derived HIEs (37).

We next investigated whether the five-day differentiated H9tHIEs would support replication of GII.4 Sydney[P31] and GII.3[P21] HuNoVs. Efficient replication of both GII genotypes was achieved (Figure 2A and 2B). A direct comparison of virus replication in the H9tHIEs and our commonly used lab prototype J2 HIE, used extensively in many studies (9), and J4*FUT2-KI* HIE lines showed that H9tHIEs supported GII.4 replication with no significant difference in viral yield when compared to the J2 and a significant reduction in viral yield when compared to the J4*FUT2-KI* line. For GII.3, there was a higher viral yield in the H9tHIE line compared to replication in the J2 HIE line, but the best replication was in the J4*FUT2-KI* HIE line. Both HuNoV strains had significant replication increases in J4*FUT-KI* compared to the J2 line.

We next evaluated viral replication in an HIE line (D_{201}HIE) generated from a duodenal biopsy obtained from a patient with common variable immunodeficiency disease (CVID) who had been suffering from chronic GII.6 HuNoV infection for years. We assessed the replication of GII.4, GII.3 and two GII.6 isolates in the differentiated D_{201}HIE line. The GII.6 virus (BCM18-1) derived from an adult CVID patient failed to replicate in this D_{201}HIE line (Figure 3), while the D_{201}HIEs supported the replication of GII.4 Sydney[P31] and GII.3[P21] with geometric mean $\log_{10}$(GE) increases of 2.7 and 2.3, respectively. The lack of replication of the patient's own virus was not likely due to the inability of this line to support GII.6 HuNoV replication because a different clinical isolate of GII.6 virus (TCH13-106) from a child hospitalized with acute gastroenteritis showed a minimal replication of 0.5 geometric mean $\log_{10}$ (GE) increase (Figure 3).

We also investigated whether the GII.6 virus inoculum from the CVID patient might not be infectious by testing replication of this virus in three other jejunal HIE lines, including the J2 HIE line and two genetically-modified J2*STAT1-KO* and J4*FUT2-KI* HIE lines made previously (30). The GII.6/CVID patient-derived virus showed minimal or no replication in J2 and J2*STAT1-KO* HIEs, respectively, but it did replicate with a geometric mean $\log_{10}$(GE) increase of 1.2 in the J4*FUT2-KI* HIE (Figure 4A). A longer replication time (72 hpi) was evaluated because of the low titer of the CVID virus inoculum. The other GII.6 isolate (TCH13-106), which replicated minimally in the D_{201}HIE line (Figure 3) was tested as a positive control and replicated in each jejunal HIE line (Figure 4B).

Next, we evaluated GII.4 and GII.3 viral replication in jejunal HIE lines (J1005 and J1006) established from specimens collected during surgery from two preterm infants, 37 and 43 weeks corrected gestational age at the time of surgical sample collection, respectively (38). Virus replication in these lines was compared to that in the prototype J2 line and the J4*FUT2-KI* HIE line. GII.4 replication in the prototype J2 was similar in the J1005 and J1006 lines. GII.4 replication was significantly higher in J4*FUT2-KI* HIEs compared to the J005 and J006 HIE lines. GII.3 replication was significantly different in J2 or J4*FUT2-KI* between all lines tested with significantly less GII.3 replication in the infant lines compared to the adult lines. Nevertheless, both GII.4 and GII.3 strains replicated in all four HIE lines tested (Figure 5).

Finally, we evaluated whether these lines exhibit quantitatively different susceptibilities to infection with the GII.4 and GII.3 viruses by determining the number of

genomic equivalents per 50% tissue culture infectious dose ($TCID_{50}$) for each virus for each line. The lowest GE/$TCID_{50}$ was seen for the GII.3 virus in the J4*FUT2-KI* HIE [3.5 (*1.01*)], [log_{10}(GE)/TCID50, standard deviation (SD)], followed by the infant HIEs [3.6 (*1.09*) and 3.6 (*1.02*) for J1005 and J1006, respectively]. Surprisingly, the GE/$TCID_{50}$ of GII.4 Sydney[P31] HuNoV was significantly higher in the J4*FUT2-KI* line [4.3 (*1.06*)] compared to J2 [3.9 (*1.07*)] and infant HIEs [3.7 (*1.05*) and 3.7 (*1.06*) for J1005 and J1006, respectively] (Table 2). To explore the specificity of this observed high GE/$TCID_{50}$ for GII.4, we tested another GII.4 Sydney strain with a different polymerase type, GII.4 Sydney[P16] (38), in this assay. The GE/$TCID_{50}$ of this strain reflected the pattern observed for GII.4 Sydney[P31], with elevated GE/$TCID_{50}$ values particularly seen in the J4*FUT2-KI* line [5.1 (*1.01*)] (Table 2).

Building upon our previous investigation where we demonstrated the successful replication of one GI genotype and 11 GII genotypes using the established HuNoV cultivation system (23), the current study demonstrates the capability of J4*FUT2-KI* to support enhanced replication of GII.4, GII.3, and GII.6 HuNoVs, as indicated by the data presented above. Based on these findings, we aimed to further elucidate the replication of additional HuNoV strains in J4*FUT2-KI* HIE monolayers. At 24 hpi, we observed an increase in viral RNA levels, with a net log_{10} difference in viral growth, ranging between 0.5 and 3.0, compared to viral RNA levels at 1-2 hpi (Table 3). By using this HIE line in our screening, we expanded the spectrum of cultivatable HuNoV strains to encompass three additional GI genotypes, GI.4, GI.5, and GI.7, and an additional GII.4 Hunter 2004 variant (Table 3, new replicating virus strains bolded).

Discussion

In our previous work, we reported conditions that enhanced the HIE culture system for HuNoV replication, marked by an expansion in the number of cultivatable strains and increased replication magnitude (23). Since then, we have established several novel HIE lines, prompting us to undertake a new evaluation to ascertain whether any of these newly established lines exhibit better performance for supporting HuNoV replication compared to our existing culture system. Additionally, the introduction of the ODM medium in 2020, by STEMCELL Technologies, raised the question about its potential to outperform the OGM media in supporting HuNoV replication.

Our comparative analysis between OGM and ODM media revealed both media support viral replication, but there was a significant enhancement in the replication efficiency of GII.4 Sydney[P31] and GII.3[P21] with OGM medium. This comparison, not previously undertaken in other studies that used OGM or ODM media (28, 39-43), provides guidance for laboratories using commercial media for HuNoV studies. Further, an evaluation of newly established lines, derived from intestinal segments of different donors, highlights strain-, donor- and segment-specific differences within the GII genogroup of HuNoVs. Varying viral replication efficiency between different intestinal segments and donors, suggests differences in receptor expression, innate immune responses, or other host factors. An unexpected result was complete lack of permissiveness for GII.3 virus replication of HIE cultures from any intestinal segment of the secretor positive 2003 donor while a GII.4 virus replicated normally in the HIEs from the small intestinal segments of this donor. The 2003 line is the first secretor positive

HIE line that we have tested that does not support GII.3 replication. Due to the limited number of small intestinal HIEs from 4 donors, we did not specifically evaluate differences in virus yields in HIEs from the distinct small intestinal segments although the data suggest there may be differences. These results support the continued testing of new lines from more donors. Such studies and more detailed studies of the 2003 line may reveal new host factors including factors that affect cell permissiveness that underlie strain-specific differences in susceptibility to HuNoV infection yet are independent of FUT2 expression and may provide new, valuable insights into the biology and pathogenesis of HuNoV infections. The lack of infection in the colonic HIEs from the same donors, where small intestinal cultures support infection, is consistent with previous histological studies that showed no detection of viral capsid protein in colon biopsies from immunocompromised patients with chronic HuNoV infection and from our previous replication studies in colonic HIEs generated from biopsies of different donors (23, 44). These new studies exclude genetics as being the factor for the lack of replication in colonic cultures.

Our studies also demonstrate that H9hESC-derived H9tHIEs support HuNoV replication. The H9hESCs are capable of differentiation into various cell types, including enteric neuronal cells or immune cells (45, 46), offering potential applications for future co-culture studies for a more comprehensive human intestinal model. The functional properties of these H9tHIE cultures may align more closely with those of human intestinal stem cell-derived HIEs, since they support efficient replication of HuNoV strains (Figure 2). Direct comparison of HuNoV replication to J2 HIEs showed that H9tHIEs provided higher viral yields, specifically for GII.3[P21]. Future studies are

needed to examine their quantitative susceptibility through a comparative assessment of $TCID_{50}$ values across multiple viral strains.

Additionally, the replication data indicate that the J4*FUT2-KI* line supports better HuNoV replication compared to the other HIE lines tested. The GII.6 CVID patient-derived virus exhibited optimal replication in J4*FUT2-KI*, with minimal observed replication in J2, and no replication observed in J2*STAT1-KO* and the patient's own HIE line. The lower titer of this virus, compared to GII.6/TCH13-106, might be a factor contributing to its poor replication. Van Kampen et al. also reported no replication of a CVID patient-derived GII.4 in the J2 line (16). It is tempting to speculate that an increased level of HBGA expression accounts for the enhanced ability of the J4*FUT2-KI* HIEs to support better replication of the GII.6 CVID (BCM18-1) or other HuNoVs (Table 3). However, the level of glycan expression in J4*FUT2-KI* HIEs is similar to that in the J2 HIE line (30), so we hypothesize that the improved replication may be linked to other altered host factors such as innate immune responses that remain to be fully understood. Studies with a CVID virus and the CVID HIE line represent opportunities to dissect biologic properties and viral evolution in a chronically infected host.

Our results confirm that infant HIE lines (38) support good GII.3 and GII.4 viral yields but these do not surpass yields in adult J2 and J*4Fut2-KI* HIE lines, as seen with another virus strain in these lines (38). Comparative assessment, based on inoculation of infant and adult HIEs revealed the J4*FUT2-KI* HIE line has a similar susceptibility to GII.3 viral infections as measured by GE/$TCID_{50}$ but infection results in higher virus yields.

Many of our studies that screen new virus strains for positive infectivity simply report the ability of an HIE line to support replication of a specific HuNoV strain in stool. We use, where possible, inocula with input GEs/well above the previously reported minimal dose needed to detect replication in HIEs for most virus strains (47). We are now further determining the GE/$TCID_{50}$ values of each inoculum to obtain comparative quantitative data on the infectivity of each virus strain in each HIE line. Determining the GE/$TCID_{50}$ values for the various virus inocula for the different HIE lines allows comparisons of the permissiveness of the different HIE lines and standardization of infections by using equivalent infectious doses (15, 48). This standardization is crucial because each stool inoculum contains different GEs and likely different particle to infectious particle ratios. This standardization also is crucial in quantitative therapeutic and comparative studies.

In these new studies, the GE/$TCID_{50}$ comparisons led to the unexpected discovery that J4*FUT2-KI* HIEs are more resistant, compared to the J2 HIE line, to infection with two distinct GII.4 Sydney strains (Table 2). While it might be expected that overexpression of FUT2 would increase susceptibility to HuNoV infection, resulting in lower TCID50 values, our findings indicate otherwise. This unexpected result for GII.4 viruses suggests that factors beyond FUT2 expression or levels of HBGA on the cell surface must influence the susceptibility of this cell culture to viral infection. Such host factors may be involved in viral entry, RNA replication or virus assembly in the J4*FUT2-KI* line. Our previous research has highlighted that compared to other HuNoVs whose entry is mediated by bile-acid induced endocytosis, GII.4 strains enter J2 HIEs by unique mechanisms (43, 49, 50). GII.4 entry and replication does not require bile acid

but involves membrane wounding, ASM-mediated lysosomal exocytosis, endosomal acidification and clathrin-independent carriers (CLIC) pathways (49), and GII.4 can overcome host interferon-mediated innate responses (51). These pathways may be different in the genetically modified J4*FUT2-KI* cultures, and further investigation is required to fully understand the molecular mechanisms responsible for the higher TCID50 values of GII.4 viruses in J4*FUT2-KI* HIEs.

Overall, the development of reliable cultivation systems for HuNoV has been a significant challenge for over five decades. Despite numerous attempts, many reported cultivation methods faced reproducibility issues (52-57). While some progress has been made in cultivating HuNoV in B cells and zebrafish models, these systems do not provide the breadth of strain coverage needed for comprehensive HuNoV research and they do not fully recapitulate host susceptibility and pathogenesis as recently reviewed (57-61). Establishment of the HIE system has significantly advanced HuNoV research by enabling cultivation of multiple HuNoV genotypes, discovery of strain-specific differences in HuNoV replication, host responses to infection, and allowing evaluation of neutralizing antibodies and therapeutics. In this study, we report successful cultivation of one additional GII and three GI genotypes, representing a substantial increase in the diversity of strains and allowing for more comparative studies and antiviral screening.

In conclusion, this study significantly provides new insight into HuNoV infection by confirming viral replication in diverse HIEs, including H9tHIEs, those from a CVID patient, organ donors, and infants. Incorporating HIEs from multiple donors reveals segment-and strain-specific susceptibility to HuNoV infection. H9tHIEs effectively mimic the human intestinal environment. We have expanded the spectrum of cultivatable

HuNoV strains, demonstrating positive replication for 4 GI and 11 GII genotypes. The J4*FUT-KI* line remains particularly promising for the growth of numerous HuNoV genotypes. Using OGM media and standardizing infections with TCID50 determinants, help ensure consistent and comparable results by providing a more accurate quantitation of the amount of GEs required for infection. These findings collectively contribute to a more robust and standardized approach to HuNoV cultivation, and continue enhancing our understanding of HuNoV biology with implications for antiviral testing and therapeutic discovery.

Materials and methods

HIES and viruses

HIE cultures used in this study are from an HIE bank maintained by Gastrointestinal Experimental Model Systems Core (GEMS) of the Texas Medical Center Digestive Diseases Center (TMC DDC) (Table 4). The use of human tissues to establish HIE cultures was approved by the Baylor College of Medicine Institutional Review Board. HIEs were generated from distinct intestinal segments from organ donors provided by the organ donation group LifeGift (Houston, TX, USA). Whole intestines were delivered on ice one hour after arrival (62). The intestinal regions were identified as follows: the duodenum was taken from the first 10 cm of the small intestine; jejunum and ileum were separated from the remaining small intestine using the vascularization of the tissue as a guide; the colon region was identified by the morphology of the colon and the patterning of mesenteric fat. Following identification and separation, the intestinal regions were washed with calcium/magnesium-free PBS buffer. HIE cultures were established from

small pieces of each intestinal region as previously described (63, 64). The D_{201}HIE line was generated from a duodenal biopsy of an individual with congenital variable immunodeficiency who was chronically infected with human norovirus. H9tHIE line was generated from H9 human Embryonic Stem Cell (H9hESC)-derived HIOs transplanted under kidney capsule of immunocompromised mice. J2*STAT-KO* and J4*FUT2-KI* HIEs are genetically modified and described previously (30). HIEs J1005 and J1006 were generated from two infants, 10 and 12 weeks at surgery (corrected gestational age, 37 and 42 weeks, respectively (65). All HIEs used in this study are secretor positive (see Table 4). Propagation of HIEs as multilobular cultures and preparation of monolayer cultures for infection were performed as previously described (23). Virus inocula were stool filtrates prepared and stored in aliquots at -80°C as previously described (9).

Media

Different media were used to maintain and differentiate HIEs:

1. A complete medium with growth factors (WRN medium), prepared at BCM by the DDC core, consisted of CMGF[−] medium (46%; v/v) (9) supplemented with mouse recombinant epidermal growth factor (EGF, 50 ng/mL final concentration; Invitrogen), nicotinamide (10 mM; Sigma), gastrin I (10 nM; Sigma), A-83-01 (500 nM; Tocris), SB202190 (10 uM; Sigma), B27 supplement (1X; Invitrogen), N2 supplement (1X; Invitrogen), *N*-acetylcysteine (1 mM; Sigma), and the conditioned medium (50%; v/v) prepared from L-WRN cell line (ATCC CRL-3276) that co-expresses Noggin, R-spondin, and Wnt-3A growth factors.
2. Commercial Intesticult human organoid growth medium (Stem Cell Technologies;

Cat#06010) is composed of two components, the OGM human basal medium and the organoid supplement. The cell pellets, resulting from HIE cell dispersion, were suspended in the proliferation OGM medium (OGMp), prepared by mixing equal volumes of basal medium and organoid supplement, and supplemented with 10 μM ROCK inhibitor Y-27632.

3. After 1 day of cell growth as a monolayer, the OGMp medium was changed to the differentiation OGM (OGMd), consisting of an equal volume of basal medium and CMGF[−] medium. The cell monolayers were differentiated for 5 days as previously described.
4. The commercial Intesticult human differentiation medium (ODM, Stem Cell Technologies; Cat# 100-0214) is another medium used to differentiate HIE monolayers.

Viral infection

Five-day differentiated HIE monolayers were washed once with CMGF(−) medium and inoculated with HuNoV for 1-2 hr at 37°C. The inoculum was removed, and monolayers were washed twice with CMGF(−) medium to remove the unbound virus. OGMd or ODM differentiation medium [100 μL containing 500 μM bile acid glycochenodeoxycholic acid (GCDCA)] was then added, and the cultures were incubated at 37°C for the indicated time points.

Tissue culture infectious dose 50% ($TCID_{50}$) assay

We determined GE/$TCID_{50}$ values to allow us to evaluate the permissiveness of each HIE line for infection with each virus and we previously reported that HuNoV strains have different GE/$TCID_{50}$ values for each HIE line (15, 48). We determined the $TCID_{50}$

411 per inoculum by examining the numbers of wells that show increases in genomic
412 equivalents of virus per well at 24 hr above baseline (at 1 hr) as measured by RT-qPCR
413 (15, 48). TCID50 per volume were calculated by Reed-Muench. We also used RT-
414 qPCR to measure the number of GEs per volume using a genogroup-specific standard.
415 We then calculated the GE per TCID50. Compiled data from 3-5 independent
416 experiments are presented. In this context, the information is expressed as the number
417 of GEs [$\log_{10}$(GE)] per TCID50) at which 50% of the cultures are infected as determined
418 by RT-qPCR.
419 Four HIE lines from 2 infants (J1005 and J1006) and 2 adults (J4*FUT2-KI*, and the
420 prototype J2) were seeded as monolayers in 96-well plate for 24 hrs in OGM
421 proliferation medium supplemented with 10 μM Rock inhibitor Y-27632, and
422 differentiated for 5 days in OGMd medium by changing the medium every other day.
423 Prior to infection, one aliquot of the GII.4 Sydney[P31] (1.8×10^7 GEs/μL), GII.4
424 Sydney[P16] (4.3×10^6 GEs/μL), or GII.3 (7.4×10^6 GEs/μL) stool samples was thawed
425 and diluted 1:5,000 in Dulbecco's phosphate buffer saline calcium/magnesium free
426 (DPBS; ThermoFisher). This viral dilution was 2-fold serially diluted in CMGF(-) basal
427 medium supplemented with 500 μM GCDCA bile acid in a 96-well round-bottom plate.
428 Six replicates were typically prepared for each dilution. HIE monolayers were then
429 infected with 100 μL of each dilution for 1 hr at 37°C under 5% CO_2 atmosphere,
430 washed twice with CMGF(-) basal medium, and incubated in 100 μL/well OGMd with
431 500 μM GCDCA. After 24 hpi, total RNA was extracted from each well and viral
432 replication was assessed by RT-qPCR in duplicate.

433 **Quantification of viral replication by RT-qPCR**

RNA extraction and RT-qPCR were performed as previously described (23). In brief, total RNA was extracted from each infected well using the KingFisher Flex purification system and MagMAX-96 Viral RNA isolation kit. RNA extracted at 1 hpi was used as a baseline to determine the amount of input virus that remained associated with cells after washing the infected cultures to remove unbound virus. The primer pair and probe COG2R/QNIF2d/QNIFS (66) were used in the RT-qPCR for detection of GII genotypes and the primer pair and probe NIFG1F/V1LCR/NIFG1P (67) were used for GI.1. RT-qPCR was performed with qScript XLT One-Step RT-qPCR ToughMix reagent with ROX reference dye (Quanta Biosciences) in an Applied Biosystems StepOnePlus thermocycler. Each extracted RNA was run in duplicate with the cycling conditions: 50°C (15 min), 95°C (5 min), followed by 40 cycles of 95°C (15 s) and 60°C (35 s). Standard curves based on recombinant GII HuNoV RNA transcripts were used to quantitate viral genome equivalents (GEs) in RNA samples. The limit of detection of the RT-qPCR assay was 20 GEs. A threshold for successful viral replication was established by considering a 0.5 increase in $\log_{10}$(GE) after 24 hpi relative to the genomic RNA detected at 1 hpi (23).

Statistical analysis

Each experiment was performed more than once, with three technical replicates of each culture condition and time point. Compiled data from at least two experiments was presented. All statistical analyses were performed on GraphPad Prism version 10.2.3 for Windows (GraphPad Software, La Jolla, CA, USA). Comparison between groups was performed using the one-way ANOVA with Tukey's multiple comparisons test or Student's t-test, which was applied to the data presented in Figure 1. *P* values of <0.05

were considered statistically significant.

Data availability

All data are available in the paper. All HIE cultures used in this study are from an HIE bank maintained by the Texas Medical Center Digestive Diseases Center (TMC DDC) core https://www.bcm.edu/research/research-centers/texas-medical-center-digestive-diseases-center.

Acknowledgements

This work was funded in part by Public Health Service grant P01-AI057788 to M.K.E, R.L.A., and BVV Prasad, P30 DK 056338 (to H. El-Serag), which supports the Texas Medical Center Digestive Diseases Center and GEMS Core, and NIH 1K08DK131326 to A.L.S. The authors acknowledge the Advanced Technology Core Laboratories (Baylor College of Medicine), specifically the Integrated Microscopy Core with funding from the NIH (DK56338, CA125123, ES030285), and 398 CPRIT (RP150578, RP170719). We thank LifeGift, Javier Nieto, and the donor families for providing intestinal tissues for generating HIEs.

Figure and table legends

Figure 1: HuNoV replication is enhanced in HIEs plated in OGM compared to ODM media.

3D J4*FUT2-KI* HIEs were propagated in WRNE media. Monolayers were seeded in OGM proliferation medium with ROCK inhibitor and differentiated in OGMd or ODM differentiation media. Differentiated monolayers were inoculated with GII.4 Sydney[P31] (9×10^5 GEs/well) or GII.3[P21] (4.3×10^5 GEs/well) diluted in CMGF(-) with 500 μM GCDCA. After 1 hpi, monolayers were washed twice and cultured in the OGMd or ODM media (+ 500 μM GCDCA). Values above the bars represent net $\log_{10}$ difference in viral growth (Δ24hr-1hr). Gray shading indicates GE at 1 hpi and purple shading shows GE at 24 hpi. Mean data compiled from two independent experiments with three wells per experiment are shown; error bars show standard deviation (SD). Experiments are denoted with different symbol shapes (circle or triangle). Significance was determined at 24 hpi using Student's *t*-test. *** p value < 0.001.

Figure 2: HuNoV replication in H9tHIEs.

Differentiated H9tHIE monolayers in OGM differentiation medium were infected with **(A)** GII.4 Sydney[P31] (9×10^5 GEs/well) or **(B)** GII.3[P21] (4.3×10^5 GEs/well) in presence of 500 μM GCDCA. After 1 hpi, monolayers were washed twice and cultured in OGM differentiation medium (+ 500 μM GCDCA). Values on bars represent the net $\log_{10}$ difference in viral growth (Δ24hr-1hr). Gray shading indicates GE at 1 hpi and blue (A) or green (B) shows GE at 24 hpi. Mean data compiled from two independent experiments with three wells per experiment are shown; error bars show SD.

Experiments are denoted by different symbol shapes (circle or triangle). Significance was determined at 24 hpi. *** p value < 0.001; ** p < 0.01; * p < 0.05.

Figure 3: HuNoV replication in D201. D201 HIE monolayers were differentiated in OGM differentiation medium and infected with GII.4/Sydney (9×10^5 GEs/well), GII.3 (4.3×10^5 GEs/well), GII.6/TCH13-106 (3.3×10^5 GEs/well) or GII.6/CVID (BCM18-1) (9.7×10^4 GEs/well) diluted in CMGF(-) supplemented with 500 μM GCDCA. After 2 hpi, monolayers were washed twice and cultured in OGM differentiation medium (+ 500 μM GCDCA). Values on bars represent net $\log_{10}$ difference in viral growth (Δ24hr-1hr). Gray shading indicates GE at 2 hpi and blue shows GE at 24 hpi. Mean data compiled from two independent experiments with three wells per experiment are shown; error bars show SD. Experiments are denoted by different symbol shapes (circle or triangle). Significance was determined at 24 hpi. *** p value < 0.001.

Figure 4: HuNoV replication in genetically modified HIEs.

HIE monolayers were differentiated in OGM differentiation medium and inoculated with **(A)** GII.6/CVID (9.7×10^4 GEs/well) or **(B)** GII.6/TCH13-106 (3.3×10^5 GEs/well) in presence of 500 μM GCDCA. After 1-2 hpi, monolayers were washed twice and cultured in OGM differentiation medium (+ 500 μM GCDCA). Values on bars represent net $\log_{10}$ difference in viral growth (Δ24hr-1hr). Gray bars indicate GE at 2 hpi and colored bars show GE at 72 hpi. Mean data compiled from two independent experiments with three wells per experiment are shown; error bars show SD. Experiments are denoted by different symbol shapes (circle or triangle). Significance was determined at 24 hpi. *** p

value < 0.001; ** p < 0.01.

Figure 5: HuNoV replication in HIEs from adults and infants. HIE monolayers were differentiated in OGM differentiation medium and infected with **(A)** GII.4/Sydney (9×10^5 GEs/well) or **(B)** GII.3 (4.3×10^5 GEs/well) diluted in CMGF(-) supplemented with 500 μM GCDCA. After 1 hpi, monolayers were washed twice and cultured in OGM differentiation medium (+ 500 μM GCDCA). Values on bars represent net $\log_{10}$ difference in viral growth (Δ24hr-1hr). Gray bars indicate GE at 1 hpi and colored bars show GE at 24 hpi. Mean data compiled from two independent experiments with three wells per experiment are shown; error bars show SD. Experiments are denoted by different symbol shapes (circle or triangle). Significance was determined at 24 hpi with significant differences between groups shown. *** p value < 0.001; ** p < 0.01.

Table 1: HuNoV yields after replication in HIEs from four donors

Differentiated monolayers were inoculated with GII.4 Sydney[P31] (9×10^5 GEs/well) or GII.3[P21] (4.3×10^5 GEs/well) diluted in CMGF(-) with 500 μM GCDCA. After 1 hpi, monolayers were washed twice and cultured in the OGMd medium (+ 500 μM GCDCA). Values represent compiled data of net $\log_{10}$ geometric mean increase in viral growth (Δ24hpi-1hpi) from 2 experiments and 3 replicate wells in each experiment; values in parentheses correspond to 95% confidence interval (95% CI).

Table 2: GE/$TCID_{50}$ values of GII.3 and GII.4 in different jejunal HIEs

Differentiated monolayers were inoculated, six wells per dilution in each experiment,

with two-fold serial dilutions of GII.4 Sydney[P31], GII.4 Sydney[P16], or GII.3[P21]. After 1 hpi, monolayers were washed twice and cultured in the OGMd medium (+ 500 µM GCDCA). * Values represent geometric mean GE/$TCID_{50}$ from n=3-5 experiments and expressed as log_{10}(GE) required to achieve infectivity of 50% of the inoculated cultures at 24 hpi; values in parentheses correspond to SD (standard deviation); superscript **[n]**: number of independent experiments.

Table 3: Cultivated HuNoV genotypes in the J4*FUT2-KI* HIE line

ND, not determined; infections with (¶) were performed in in-house media; infections without (¶) were performed in OGM media; Bolded strains have not been reported before; all infections were conducted in the presence of GCDCA.

Table 4: HIE lines used in this study

Se, secretor; Le, Lewis; y, years; wks, weeks; D, duodenum; J, jejunum, I, ileum; C, colon; (•): H9tHIE were generated from 8-week-old tHIOs which are developmentally similar to an 18 gestational week human fetal intestine (36); (••): (age at surgery/corrected gestational age at surgery).

References

1. Atmar RL, Ramani S, Estes MK. Human noroviruses: recent advances in a 50-year history. Current opinion in infectious diseases. 2018;31(5):422-32. Epub 2018/08/14. doi: 10.1097/qco.0000000000000476. PubMed PMID: 30102614.
2. de Graaf M, van Beek J, Koopmans MPG. Human norovirus transmission and evolution in a changing world. Nature Reviews Microbiology. 2016;14(7):421-33. doi: 10.1038/nrmicro.2016.48.
3. Green KY. Norovirus infection in immunocompromised hosts. Clinical microbiology and infection : the official publication of the European Society of Clinical

Microbiology and Infectious Diseases. 2014;20(8):717-23. Epub 2014/07/22. doi: 10.1111/1469-0691.12761. PubMed PMID: 25040790.

4. Pires SM, Fischer-Walker CL, Lanata CF, Devleesschauwer B, Hall AJ, Kirk MD, Duarte AS, Black RE, Angulo FJ. Aetiology-Specific Estimates of the Global and Regional Incidence and Mortality of Diarrhoeal Diseases Commonly Transmitted through Food. PloS one. 2015;10(12):e0142927. Epub 2015/12/04. doi: 10.1371/journal.pone.0142927. PubMed PMID: 26632843; PMCID: PMC4668836.
5. Bartsch SM, Lopman BA, Ozawa S, Hall AJ, Lee BY. Global Economic Burden of Norovirus Gastroenteritis. PloS one. 2016;11(4):e0151219. Epub 2016/04/27. doi: 10.1371/journal.pone.0151219. PubMed PMID: 27115736; PMCID: PMC4846012.
6. Bartsch SM, O'Shea KJ, Lee BY. The Clinical and Economic Burden of Norovirus Gastroenteritis in the United States. The Journal of infectious diseases. 2020;222(11):1910-9. Epub 2020/07/17. doi: 10.1093/infdis/jiaa292. PubMed PMID: 32671397; PMCID: PMC8171800.
7. Debbink K, Lindesmith LC, Baric RS. The state of norovirus vaccines. Clinical infectious diseases : an official publication of the Infectious Diseases Society of America. 2014;58(12):1746-52. Epub 2014/03/04. doi: 10.1093/cid/ciu120. PubMed PMID: 24585561; PMCID: PMC4036685.
8. Prasad BV, Shanker S, Muhaxhiri Z, Deng L, Choi JM, Estes MK, Song Y, Palzkill T, Atmar RL. Antiviral targets of human noroviruses. Current opinion in virology. 2016;18:117-25. Epub 2016/06/20. doi: 10.1016/j.coviro.2016.06.002. PubMed PMID: 27318434; PMCID: PMC4983487.
9. Ettayebi K, Crawford SE, Murakami K, Broughman JR, Karandikar U, Tenge VR, Neill FH, Blutt SE, Zeng XL, Qu L, Kou B, Opekun AR, Burrin D, Graham DY, Ramani S, Atmar RL, Estes MK. Replication of human noroviruses in stem cell-derived human enteroids. Science (New York, NY). 2016;353(6306):1387-93. Epub 2016/08/27. doi: 10.1126/science.aaf5211. PubMed PMID: 27562956; PMCID: PMC5305121.
10. Alvarado G, Salmen W, Ettayebi K, Hu L, Sankaran B, Estes MK, Venkataram Prasad BV, Crowe JE, Jr. Broadly cross-reactive human antibodies that inhibit genogroup I and II noroviruses. Nature communications. 2021;12(1):4320. Epub 2021/07/16. doi: 10.1038/s41467-021-24649-w. PubMed PMID: 34262046; PMCID: PMC8280134.
11. Ettayebi K, Salmen W, Imai K, Hagi A, Neill FH, Atmar RL, Prasad BVV, Estes MK. Antiviral Activity of Olanexidine-Containing Hand Rub against Human Noroviruses. mBio. 2022;13(2):e0284821. Epub 2022/03/18. doi: 10.1128/mbio.02848-21. PubMed PMID: 35297675; PMCID: PMC9040745.
12. Alvarado G, Ettayebi K, Atmar RL, Bombardi RG, Kose N, Estes MK, Crowe JE, Jr. Human Monoclonal Antibodies That Neutralize Pandemic GII.4 Noroviruses. Gastroenterology. 2018;155(6):1898-907. Epub 2018/09/01. doi: 10.1053/j.gastro.2018.08.039. PubMed PMID: 30170116; PMCID: PMC6402321.
13. Atmar RL, Ettayebi K, Ayyar BV, Neill FH, Braun RP, Ramani S, Estes MK. Comparison of Microneutralization and Histo-Blood Group Antigen-Blocking Assays for Functional Norovirus Antibody Detection. The Journal of infectious diseases. 2020;221(5):739-43. Epub 2019/10/16. doi: 10.1093/infdis/jiz526. PubMed PMID: 31613328; PMCID: PMC8483564.

14. Costantini V, Morantz EK, Browne H, Ettayebi K, Zeng XL, Atmar RL, Estes MK, Vinjé J. Human Norovirus Replication in Human Intestinal Enteroids as Model to Evaluate Virus Inactivation. Emerging infectious diseases. 2018;24(8):1453-64. Epub 2018/07/18. doi: 10.3201/eid2408.180126. PubMed PMID: 30014841; PMCID: PMC6056096.
15. Lewis MA, Cortés-Penfield NW, Ettayebi K, Patil K, Kaur G, Neill FH, Atmar RL, Ramani S, Estes MK. Standardization of an antiviral pipeline for human norovirus in human intestinal enteroids demonstrates nitazoxanide has no to weak antiviral activity. Antimicrobial agents and chemotherapy. 2023;67(10):e0063623. Epub 2023/10/03. doi: 10.1128/aac.00636-23. PubMed PMID: 37787556; PMCID: PMC10583671.
16. van Kampen JJA, Dalm V, Fraaij PLA, Oude Munnink BB, Schapendonk CME, Izquierdo-Lara RW, Villabruna N, Ettayebi K, Estes MK, Koopmans MPG, de Graaf M. Clinical and In Vitro Evidence Favoring Immunoglobulin Treatment of a Chronic Norovirus Infection in a Patient With Common Variable Immunodeficiency. The Journal of infectious diseases. 2022;226(10):1781-9. Epub 2022/03/08. doi: 10.1093/infdis/jiac085. PubMed PMID: 35255136; PMCID: PMC9650502.
17. Salmen W, Hu L, Bok M, Chaimongkol N, Ettayebi K, Sosnovtsev SV, Soni K, Ayyar BV, Shanker S, Neill FH, Sankaran B, Atmar RL, Estes MK, Green KY, Parreño V, Prasad BVV. A single nanobody neutralizes multiple epochally evolving human noroviruses by modulating capsid plasticity. Nature communications. 2023;14(1):6516. Epub 2023/10/17. doi: 10.1038/s41467-023-42146-0. PubMed PMID: 37845211; PMCID: PMC10579229.
18. Hayashi T, Murakami K, Hirano J, Fujii Y, Yamaoka Y, Ohashi H, Watashi K, Estes MK, Muramatsu M. Dasabuvir Inhibits Human Norovirus Infection in Human Intestinal Enteroids. mSphere. 2021;6(6):e0062321. Epub 2021/11/04. doi: 10.1128/mSphere.00623-21. PubMed PMID: 34730374; PMCID: PMC8565515.
19. Mirabelli C, Santos-Ferreira N, Gillilland MG, 3rd, Cieza RJ, Colacino JA, Sexton JZ, Neyts J, Taube S, Rocha-Pereira J, Wobus CE. Human Norovirus Efficiently Replicates in Differentiated 3D-Human Intestinal Enteroids. Journal of virology. 2022;96(22):e0085522. Epub 2022/11/08. doi: 10.1128/jvi.00855-22. PubMed PMID: 36342297; PMCID: PMC9683019.
20. Ford-Siltz LA, Tohma K, Alvarado GS, Kendra JA, Pilewski KA, Crowe JE, Jr., Parra GI. Cross-reactive neutralizing human monoclonal antibodies mapping to variable antigenic sites on the norovirus major capsid protein. Frontiers in immunology. 2022;13:1040836. Epub 2022/11/18. doi: 10.3389/fimmu.2022.1040836. PubMed PMID: 36389818; PMCID: PMC9641292.
21. Lindesmith LC, McDaniel JR, Changela A, Verardi R, Kerr SA, Costantini V, Brewer-Jensen PD, Mallory ML, Voss WN, Boutz DR, Blazeck JJ, Ippolito GC, Vinje J, Kwong PD, Georgiou G, Baric RS. Sera Antibody Repertoire Analyses Reveal Mechanisms of Broad and Pandemic Strain Neutralizing Responses after Human Norovirus Vaccination. Immunity. 2019;50(6):1530-41.e8. Epub 2019/06/20. doi: 10.1016/j.immuni.2019.05.007. PubMed PMID: 31216462; PMCID: PMC6591005.
22. Koromyslova AD, Morozov VA, Hefele L, Hansman GS. Human Norovirus Neutralized by a Monoclonal Antibody Targeting the Histo-Blood Group Antigen

Pocket. Journal of virology. 2019;93(5). Epub 2018/12/14. doi: 10.1128/jvi.02174-18. PubMed PMID: 30541855; PMCID: PMC6384083.

23. Ettayebi K, Tenge VR, Cortes-Penfield NW, Crawford SE, Neill FH, Zeng XL, Yu X, Ayyar BV, Burrin D, Ramani S, Atmar RL, Estes MK. New Insights and Enhanced Human Norovirus Cultivation in Human Intestinal Enteroids. mSphere. 2021;6(1). Epub 2021/01/29. doi: 10.1128/mSphere.01136-20. PubMed PMID: 33504663; PMCID: PMC7885322.
24. Atmar RL, Ettayebi K, Ramani S, Neill FH, Lindesmith L, Baric RS, Brinkman A, Braun R, Sherwood J, Estes MK. A Bivalent Human Norovirus Vaccine Induces Homotypic and Heterotypic Neutralizing Antibodies. The Journal of infectious diseases. 2023. Epub 2023/10/02. doi: 10.1093/infdis/jiad401. PubMed PMID: 37781879.
25. Mboko WP, Chhabra P, Valcarce MD, Costantini V, Vinjé J. Advances in understanding of the innate immune response to human norovirus infection using organoid models. The Journal of general virology. 2022;103(1). Epub 2022/01/26. doi: 10.1099/jgv.0.001720. PubMed PMID: 35077345; PMCID: PMC8984994.
26. Chan JCM, Mohammad KN, Zhang LY, Wong SH, Chan MC. Targeted Profiling of Immunological Genes during Norovirus Replication in Human Intestinal Enteroids. Viruses. 2021;13(2). Epub 2021/01/27. doi: 10.3390/v13020155. PubMed PMID: 33494515; PMCID: PMC7910953.
27. Hosmillo M, Chaudhry Y, Nayak K, Sorgeloos F, Koo BK, Merenda A, Lillestol R, Drumright L, Zilbauer M, Goodfellow I. Norovirus Replication in Human Intestinal Epithelial Cells Is Restricted by the Interferon-Induced JAK/STAT Signaling Pathway and RNA Polymerase II-Mediated Transcriptional Responses. mBio. 2020;11(2). Epub 2020/03/19. doi: 10.1128/mBio.00215-20. PubMed PMID: 32184238; PMCID: PMC7078467.
28. Hayashi T, Murakami K, Ando H, Ueno S, Kobayashi S, Muramatsu M, Tanikawa T, Kitamura M. Inhibitory effect of Ephedra herba on human norovirus infection in human intestinal organoids. Biochemical and biophysical research communications. 2023;671:200-4. Epub 2023/06/12. doi: 10.1016/j.bbrc.2023.05.127. PubMed PMID: 37302295.
29. Carmona-Vicente N, Pandiscia A, Santiso-Bellón C, Perez-Cataluña A, Rodríguez-Díaz J, Costantini VP, Buesa J, Vinjé J, Sánchez G, Randazzo W. Human intestinal enteroids platform to assess the infectivity of gastroenteritis viruses in wastewater. Water research. 2024;255:121481. Epub 2024/03/24. doi: 10.1016/j.watres.2024.121481. PubMed PMID: 38520776.
30. Haga K, Ettayebi K, Tenge VR, Karandikar UC, Lewis MA, Lin SC, Neill FH, Ayyar BV, Zeng XL, Larson G, Ramani S, Atmar RL, Estes MK. Genetic Manipulation of Human Intestinal Enteroids Demonstrates the Necessity of a Functional Fucosyltransferase 2 Gene for Secretor-Dependent Human Norovirus Infection. mBio. 2020;11(2). Epub 2020/03/19. doi: 10.1128/mBio.00251-20. PubMed PMID: 32184242; PMCID: PMC7078471.
31. Spence JR, Mayhew CN, Rankin SA, Kuhar MF, Vallance JE, Tolle K, Hoskins EE, Kalinichenko VV, Wells SI, Zorn AM, Shroyer NF, Wells JM. Directed differentiation of human pluripotent stem cells into intestinal tissue in vitro. Nature.

2011;470(7332):105-9. Epub 2010/12/15. doi: 10.1038/nature09691. PubMed PMID: 21151107; PMCID: PMC3033971.

32. Finkbeiner SR, Hill DR, Altheim CH, Dedhia PH, Taylor MJ, Tsai YH, Chin AM, Mahe MM, Watson CL, Freeman JJ, Nattiv R, Thomson M, Klein OD, Shroyer NF, Helmrath MA, Teitelbaum DH, Dempsey PJ, Spence JR. Transcriptome-wide Analysis Reveals Hallmarks of Human Intestine Development and Maturation In Vitro and In Vivo. Stem cell reports. 2015;4(6):1140-55. Epub 2015/06/09. doi: 10.1016/j.stemcr.2015.04.010. PubMed PMID: 26050928; PMCID: PMC4471827.
33. Boyle MA, Sequeira DJ, McNeill EP, Criss ZK, 2nd, Shroyer NF, Speer AL. In Vivo Transplantation of Human Intestinal Organoids Enhances Select Tight Junction Gene Expression. The Journal of surgical research. 2021;259:500-8. Epub 2020/11/11. doi: 10.1016/j.jss.2020.10.002. PubMed PMID: 33168233; PMCID: PMC8634850.
34. Bouffi C, Wikenheiser-Brokamp KA, Chaturvedi P, Sundaram N, Goddard GR, Wunderlich M, Brown NE, Staab JF, Latanich R, Zachos NC, Holloway EM, Mahe MM, Poling HM, Vales S, Fisher GW, Spence JR, Mulloy JC, Zorn AM, Wells JM, Helmrath MA. In vivo development of immune tissue in human intestinal organoids transplanted into humanized mice. Nature biotechnology. 2023. Epub 2023/01/27. doi: 10.1038/s41587-022-01558-x. PubMed PMID: 36702898.
35. Watson CL, Mahe MM, Múnera J, Howell JC, Sundaram N, Poling HM, Schweitzer JI, Vallance JE, Mayhew CN, Sun Y, Grabowski G, Finkbeiner SR, Spence JR, Shroyer NF, Wells JM, Helmrath MA. An in vivo model of human small intestine using pluripotent stem cells. Nature medicine. 2014;20(11):1310-4. Epub 2014/10/20. doi: 10.1038/nm.3737. PubMed PMID: 25326803; PMCID: PMC4408376.
36. Singh A, Poling HM, Chaturvedi P, Thorner K, Sundaram N, Kechele DO, Childs CJ, McCauley HA, Fisher GW, Brown NE, Spence JR, Wells JM, Helmrath MA. Transplanted human intestinal organoids: a resource for modeling human intestinal development. Development (Cambridge, England). 2023;150(9). Epub 2023/04/19. doi: 10.1242/dev.201416. PubMed PMID: 37070767; PMCID: PMC10259511.
37. Sato T, Vries RG, Snippert HJ, van de Wetering M, Barker N, Stange DE, van Es JH, Abo A, Kujala P, Peters PJ, Clevers H. Single Lgr5 stem cells build crypt-villus structures in vitro without a mesenchymal niche. Nature. 2009;459(7244):262-5. Epub 2009/03/31. doi: 10.1038/nature07935. PubMed PMID: 19329995.
38. Adeniyi-Ipadeola GO, Hankins JD, Kambal A, Zeng XL, Patil K, Poplaski V, Bomidi C, Nguyen-Phuc H, Grimm SL, Coarfa C, Stossi F, Crawford SE, Blutt SE, Speer AL, Estes MK, Ramani S. Infant and adult human intestinal enteroids are morphologically and functionally distinct. mBio. 2024;15(8):e0131624. Epub 2024/07/02. doi: 10.1128/mbio.01316-24. PubMed PMID: 38953637; PMCID: PMC11323560.
39. Hayashi T, Yamaoka Y, Ito A, Kamaishi T, Sugiyama R, Estes MK, Muramatsu M, Murakami K. Evaluation of Heat Inactivation of Human Norovirus in Freshwater Clams Using Human Intestinal Enteroids. Viruses. 2022;14(5). Epub 2022/05/29. doi: 10.3390/v14051014. PubMed PMID: 35632754; PMCID: PMC9146323.
40. Euller-Nicolas G, Le Mennec C, Schaeffer J, Zeng XL, Ettayebi K, Atmar RL, Le Guyader FS, Estes MK, Desdouits M. Human Sapovirus Replication in Human

Intestinal Enteroids. Journal of virology. 2023;97(4):e0038323. Epub 2023/04/12. doi: 10.1128/jvi.00383-23. PubMed PMID: 37039654; PMCID: PMC10134857.

41. Narwankar R, Esseili MA. Replication of Human Norovirus in Human Intestinal Enteroids Is Affected by Fecal Sample Processing. Viruses. 2024;16(2). Epub 2024/02/24. doi: 10.3390/v16020241. PubMed PMID: 38400017; PMCID: PMC10893307.
42. Santos-Ferreira N, Van Dycke J, Chiu W, Neyts J, Matthijnssens J, Rocha-Pereira J. Molnupiravir inhibits human norovirus and rotavirus replication in 3D human intestinal enteroids. Antiviral research. 2024;223:105839. Epub 2024/02/20. doi: 10.1016/j.antiviral.2024.105839. PubMed PMID: 38373532.
43. Tenge V, Vijayalakshmi Ayyar B, Ettayebi K, Crawford SE, Shen YT, Neill FH, Atmar RL, Estes MK. Bile acid-sensitive human norovirus strains are susceptible to sphingosine-1-phosphate receptor 2 inhibition. bioRxiv : the preprint server for biology. 2024. Epub 2024/01/23. doi: 10.1101/2024.01.02.573926. PubMed PMID: 38260626; PMCID: PMC10802320.
44. Karandikar UC, Crawford SE, Ajami NJ, Murakami K, Kou B, Ettayebi K, Papanicolaou GA, Jongwutiwes U, Perales MA, Shia J, Mercer D, Finegold MJ, Vinjé J, Atmar RL, Estes MK. Detection of human norovirus in intestinal biopsies from immunocompromised transplant patients. The Journal of general virology. 2016;97(9):2291-300. Epub 2016/07/15. doi: 10.1099/jgv.0.000545. PubMed PMID: 27412790; PMCID: PMC5756488.
45. Workman MJ, Mahe MM, Trisno S, Poling HM, Watson CL, Sundaram N, Chang CF, Schiesser J, Aubert P, Stanley EG, Elefanty AG, Miyaoka Y, Mandegar MA, Conklin BR, Neunlist M, Brugmann SA, Helmrath MA, Wells JM. Engineered human pluripotent-stem-cell-derived intestinal tissues with a functional enteric nervous system. Nature medicine. 2017;23(1):49-59. Epub 2016/11/22. doi: 10.1038/nm.4233. PubMed PMID: 27869805; PMCID: PMC5562951.
46. Estridge RC, O'Neill JE, Keung AJ. Matrigel Tunes H9 Stem Cell-Derived Human Cerebral Organoid Development. Organoids. 2023;2(4):165-76. Epub 2024/01/10. doi: 10.3390/organoids2040013. PubMed PMID: 38196836; PMCID: PMC10776236.
47. Estes MK, Ettayebi K, Tenge VR, Murakami K, Karandikar U, Lin SC, Ayyar BV, Cortes-Penfield NW, Haga K, Neill FH, Opekun AR, Broughman JR, Zeng XL, Blutt SE, Crawford SE, Ramani S, Graham DY, Atmar RL. Human Norovirus Cultivation in Nontransformed Stem Cell-Derived Human Intestinal Enteroid Cultures: Success and Challenges. Viruses. 2019;11(7). Epub 2019/07/25. doi: 10.3390/v11070638. PubMed PMID: 31336765; PMCID: PMC6669637.
48. Lewis MA, Patil K, Ettayebi K, Estes MK, Atmar RL, Ramani S. Divergent responses of human intestinal organoid monolayers using commercial in vitro cytotoxicity assays. PloS one. 2024;19(6):e0304526. Epub 2024/06/10. doi: 10.1371/journal.pone.0304526. PubMed PMID: 38857221; PMCID: PMC11164375.
49. Ayyar BV, Ettayebi K, Salmen W, Karandikar UC, Neill FH, Tenge VR, Crawford SE, Bieberich E, Prasad BVV, Atmar RL, Estes MK. CLIC and membrane wound repair pathways enable pandemic norovirus entry and infection. Nature communications. 2023;14(1):1148. Epub 2023/03/01. doi: 10.1038/s41467-023-36398-z. PubMed PMID: 36854760; PMCID: PMC9974061.

50. Murakami K, Tenge VR, Karandikar UC, Lin SC, Ramani S, Ettayebi K, Crawford SE, Zeng XL, Neill FH, Ayyar BV, Katayama K, Graham DY, Bieberich E, Atmar RL, Estes MK. Bile acids and ceramide overcome the entry restriction for GII.3 human norovirus replication in human intestinal enteroids. Proceedings of the National Academy of Sciences of the United States of America. 2020;117(3):1700-10. Epub 2020/01/04. doi: 10.1073/pnas.1910138117. PubMed PMID: 31896578; PMCID: PMC6983410.
51. Lin SC, Qu L, Ettayebi K, Crawford SE, Blutt SE, Robertson MJ, Zeng XL, Tenge VR, Ayyar BV, Karandikar UC, Yu X, Coarfa C, Atmar RL, Ramani S, Estes MK. Human norovirus exhibits strain-specific sensitivity to host interferon pathways in human intestinal enteroids. Proceedings of the National Academy of Sciences of the United States of America. 2020;117(38):23782-93. Epub 2020/09/11. doi: 10.1073/pnas.2010834117. PubMed PMID: 32907944; PMCID: PMC7519316.
52. Herbst-Kralovetz MM, Radtke AL, Lay MK, Hjelm BE, Bolick AN, Sarker SS, Atmar RL, Kingsley DH, Arntzen CJ, Estes MK, Nickerson CA. Lack of norovirus replication and histo-blood group antigen expression in 3-dimensional intestinal epithelial cells. Emerging infectious diseases. 2013;19(3):431-8. Epub 2013/04/30. doi: 10.3201/eid1903.121029. PubMed PMID: 23622517; PMCID: PMC3647661.
53. Papafragkou E, Hewitt J, Park GW, Greening G, Vinjé J. Challenges of culturing human norovirus in three-dimensional organoid intestinal cell culture models. PloS one. 2014;8(6):e63485. Epub 2013/06/12. doi: 10.1371/journal.pone.0063485. PubMed PMID: 23755105; PMCID: PMC3670855.
54. Straub TM, Höner zu Bentrup K, Orosz-Coghlan P, Dohnalkova A, Mayer BK, Bartholomew RA, Valdez CO, Bruckner-Lea CJ, Gerba CP, Abbaszadegan M, Nickerson CA. In vitro cell culture infectivity assay for human noroviruses. Emerging infectious diseases. 2007;13(3):396-403. Epub 2007/06/08. doi: 10.3201/eid1303.060549. PubMed PMID: 17552092; PMCID: PMC2725917.
55. Takanashi S, Saif LJ, Hughes JH, Meulia T, Jung K, Scheuer KA, Wang Q. Failure of propagation of human norovirus in intestinal epithelial cells with microvilli grown in three-dimensional cultures. Archives of virology. 2014;159(2):257-66. Epub 2013/08/27. doi: 10.1007/s00705-013-1806-4. PubMed PMID: 23974469; PMCID: PMC3946686.
56. Straub TM, Hutchison JR, Bartholomew RA, Valdez CO, Valentine NB, Dohnalkova A, Ozanich RM, Bruckner-Lea CJ. Defining cell culture conditions to improve human norovirus infectivity assays. Water science and technology : a journal of the International Association on Water Pollution Research. 2013;67(4):863-8. Epub 2013/01/12. doi: 10.2166/wst.2012.636. PubMed PMID: 23306266.
57. Jones MK, Grau KR, Costantini V, Kolawole AO, de Graaf M, Freiden P, Graves CL, Koopmans M, Wallet SM, Tibbetts SA, Schultz-Cherry S, Wobus CE, Vinjé J, Karst SM. Human norovirus culture in B cells. Nature protocols. 2015;10(12):1939-47. Epub 2015/10/30. doi: 10.1038/nprot.2015.121. PubMed PMID: 26513671; PMCID: PMC4689599.
58. Jones MK, Watanabe M, Zhu S, Graves CL, Keyes LR, Grau KR, Gonzalez-Hernandez MB, Iovine NM, Wobus CE, Vinjé J, Tibbetts SA, Wallet SM, Karst SM. Enteric bacteria promote human and mouse norovirus infection of B cells. Science

(New York, NY). 2014;346(6210):755-9. Epub 2014/11/08. doi: 10.1126/science.1257147. PubMed PMID: 25378626; PMCID: PMC4401463.

59. Van Dycke J, Ny A, Conceição-Neto N, Maes J, Hosmillo M, Cuvry A, Goodfellow I, Nogueira TC, Verbeken E, Matthijnssens J, de Witte P, Neyts J, Rocha-Pereira J. A robust human norovirus replication model in zebrafish larvae. PLoS pathogens. 2019;15(9):e1008009. Epub 2019/09/20. doi: 10.1371/journal.ppat.1008009. PubMed PMID: 31536612; PMCID: PMC6752765.
60. Van Dycke J, Cuvry A, Knickmann J, Ny A, Rakers S, Taube S, de Witte P, Neyts J, Rocha-Pereira J. Infection of zebrafish larvae with human norovirus and evaluation of the in vivo efficacy of small-molecule inhibitors. Nature protocols. 2021;16(4):1830-49. Epub 2021/04/11. doi: 10.1038/s41596-021-00499-0. PubMed PMID: 33837302.
61. Hayashi T, Kobayashi S, Hirano J, Murakami K. Human norovirus cultivation systems and their use in antiviral research. Journal of virology. 2024;98(4):e0166323. Epub 2024/03/12. doi: 10.1128/jvi.01663-23. PubMed PMID: 38470106; PMCID: PMC11019851.
62. Danhof HA, Lee J, Thapa A, Britton RA, Di Rienzi SC. Microbial stimulation of oxytocin release from the intestinal epithelium via secretin signaling. bioRxiv : the preprint server for biology. 2023. Epub 2023/03/23. doi: 10.1101/2023.03.09.531917. PubMed PMID: 36945649; PMCID: PMC10028957 provisional patent (HAD, RAB, SCD).
63. Zou WY, Blutt SE, Crawford SE, Ettayebi K, Zeng XL, Saxena K, Ramani S, Karandikar UC, Zachos NC, Estes MK. Human Intestinal Enteroids: New Models to Study Gastrointestinal Virus Infections. Methods in molecular biology (Clifton, NJ). 2019;1576:229-47. Epub 2017/04/01. doi: 10.1007/7651_2017_1. PubMed PMID: 28361480; PMCID: PMC5752619.
64. Sato T, Stange DE, Ferrante M, Vries RG, Van Es JH, Van den Brink S, Van Houdt WJ, Pronk A, Van Gorp J, Siersema PD, Clevers H. Long-term expansion of epithelial organoids from human colon, adenoma, adenocarcinoma, and Barrett's epithelium. Gastroenterology. 2011;141(5):1762-72. Epub 2011/09/06. doi: 10.1053/j.gastro.2011.07.050. PubMed PMID: 21889923.
65. Adeniyi-Ipadeola GO, Hankins JD, Kambal A, Zeng XL, Patil K, Poplaski V, Bomidi C, Nguyen-Phuc H, Grimm SL, Coarfa C, Crawford SE, Blutt SE, Speer AL, Estes MK, Ramani S. Infant and Adult Human Intestinal Enteroids are Morphologically and Functionally Distinct. bioRxiv : the preprint server for biology. 2023. Epub 2023/06/09. doi: 10.1101/2023.05.19.541350. PubMed PMID: 37292968; PMCID: PMC10245709.
66. Loisy F, Atmar RL, Guillon P, Le Cann P, Pommepuy M, Le Guyader FS. Real-time RT-PCR for norovirus screening in shellfish. Journal of virological methods. 2005;123(1):1-7. Epub 2004/12/08. doi: 10.1016/j.jviromet.2004.08.023. PubMed PMID: 15582692.
67. Miura T, Parnaudeau S, Grodzki M, Okabe S, Atmar RL, Le Guyader FS. Environmental detection of genogroup I, II, and IV noroviruses by using a generic real-time reverse transcription-PCR assay. Applied and environmental microbiology. 2013;79(21):6585-92. Epub 2013/08/21. doi: 10.1128/aem.02112-13. PubMed PMID: 23956397; PMCID: PMC3811514.

895

896

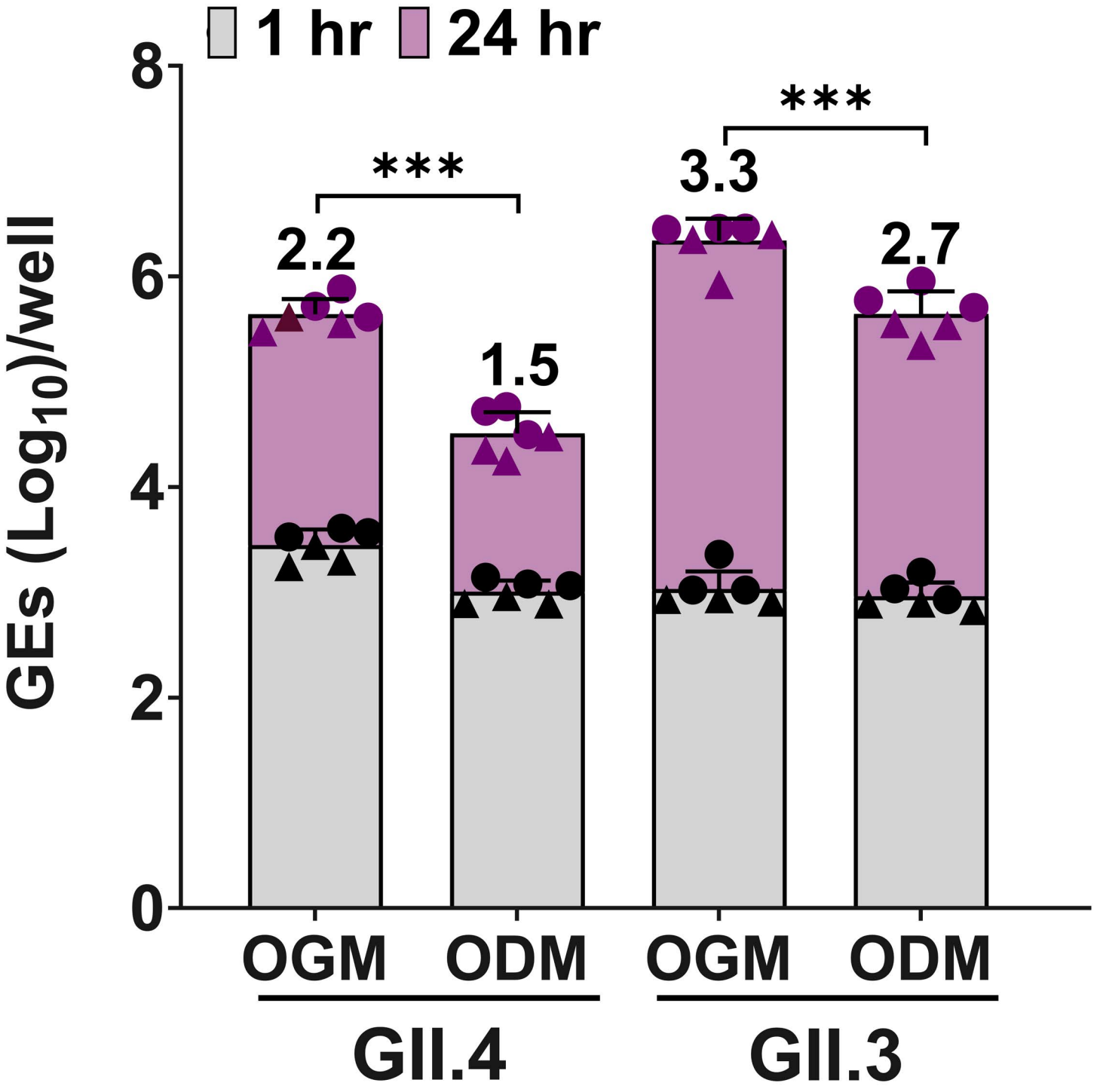
1 hr
24 hr
GEs (Log10)/well
8
6
4
2
0
***
***
2.2
1.5
3.3
2.7
OGM
ODM
OGM
ODM
GII.4
GII.3

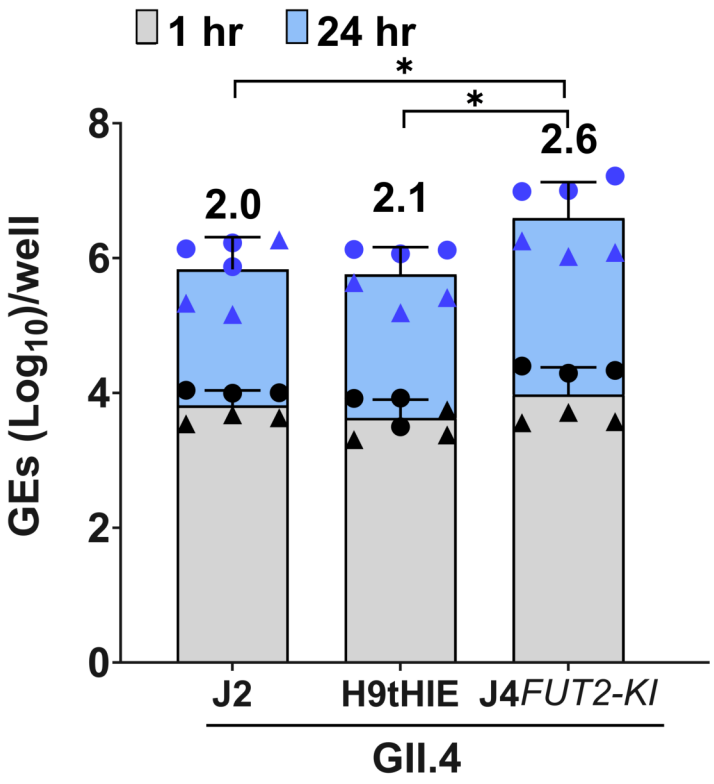
1 hr
24 hr
*
*
2.0
2.1
2.6
GEs (Log10)/well
0
2
4
6
8
J2
H9tHIE
J4FUT2-KI
GII.4

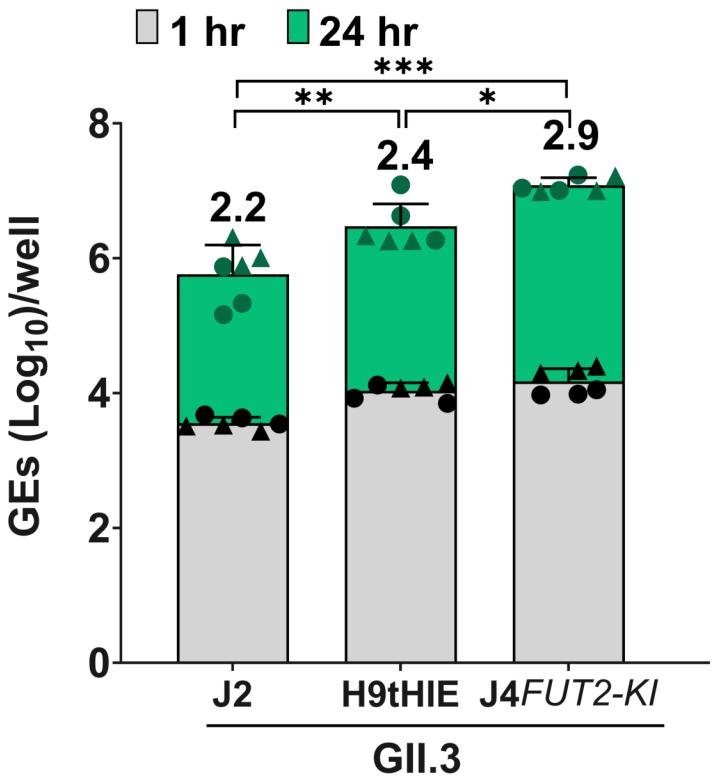
1 hr
24 hr
***
**
*
2.2
2.4
2.9
GEs (Log10)/well
0
2
4
6
8
J2
H9tHIE
J4FUT2-KI
GII.3

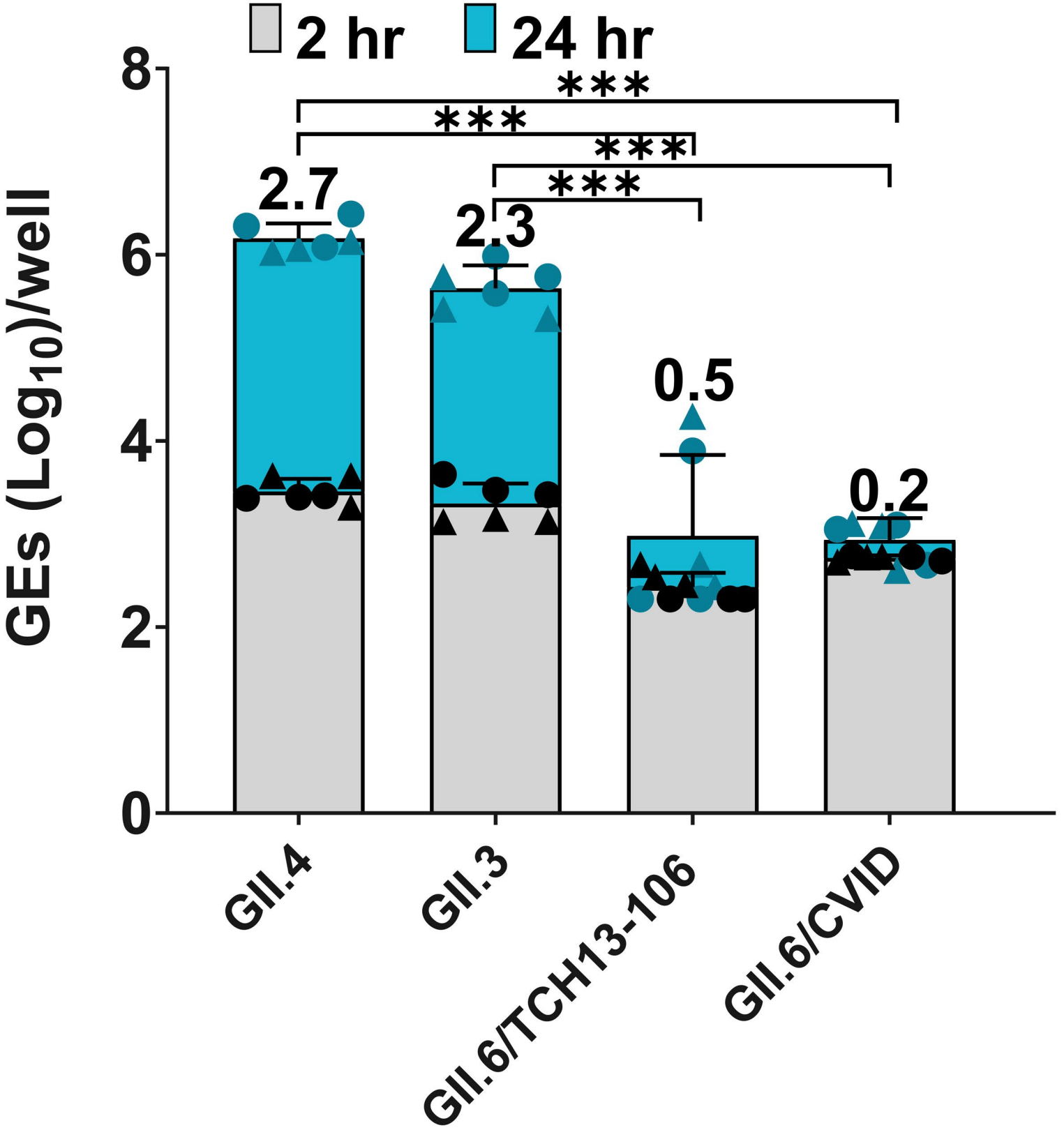
2 hr
24 hr
GEs (Log10)/well
8
6
4
2
0
***
***
***
***
2.7
2.3
0.5
0.2
GII.4
GII.3
GII.6/TCH13-106
GII.6/CVID

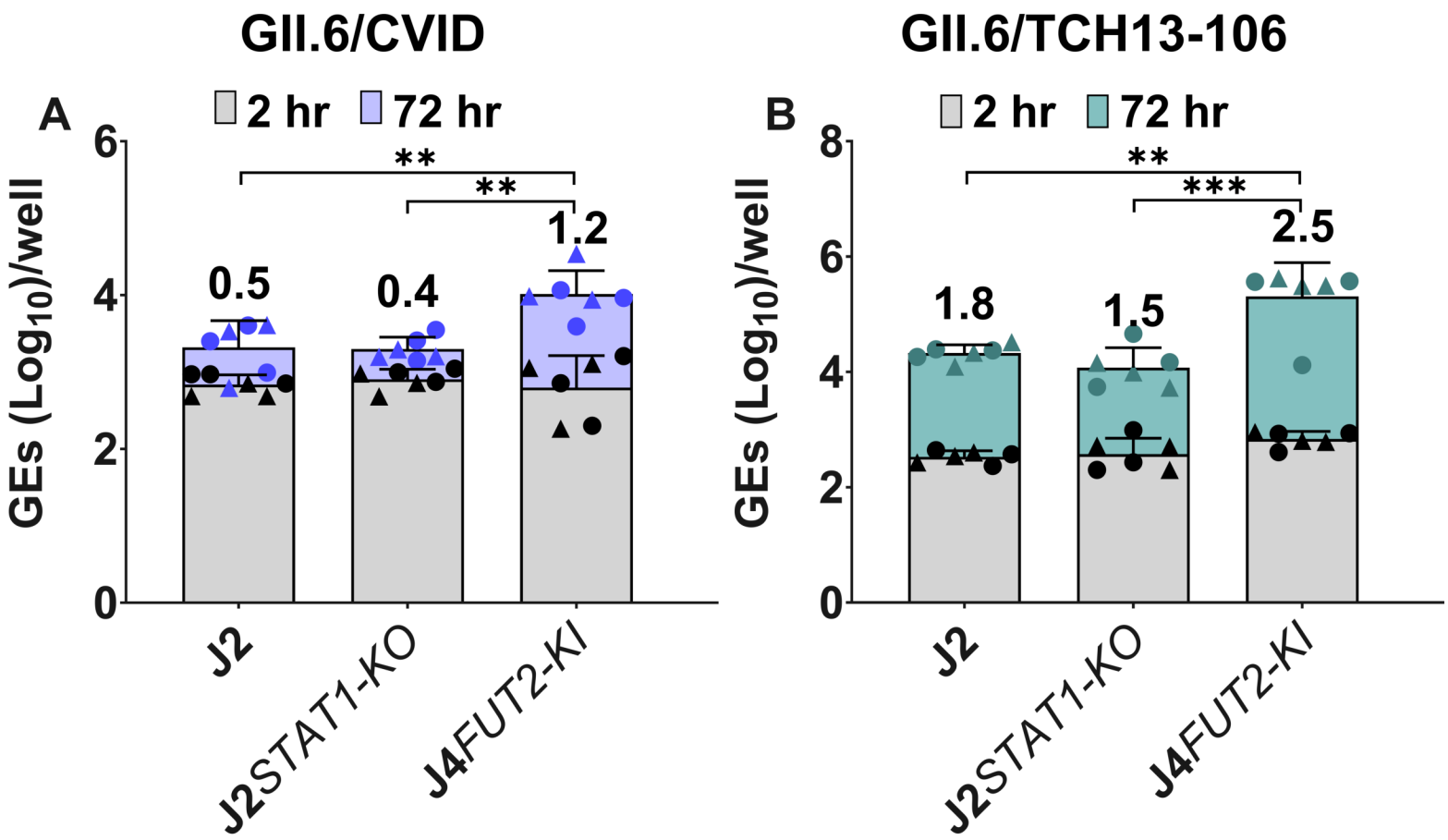
GII.6/CVID
A
2 hr
72 hr
GEs (Log10)/well
0
2
4
6
**
**
0.5
0.4
1.2
J2
J2STAT1-KO
J4FUT2-KI
GII.6/TCH13-106
B
2 hr
72 hr
GEs (Log10)/well
0
2
4
6
8
**
***
1.8
1.5
2.5
J2
J2STAT1-KO
J4FUT2-KI

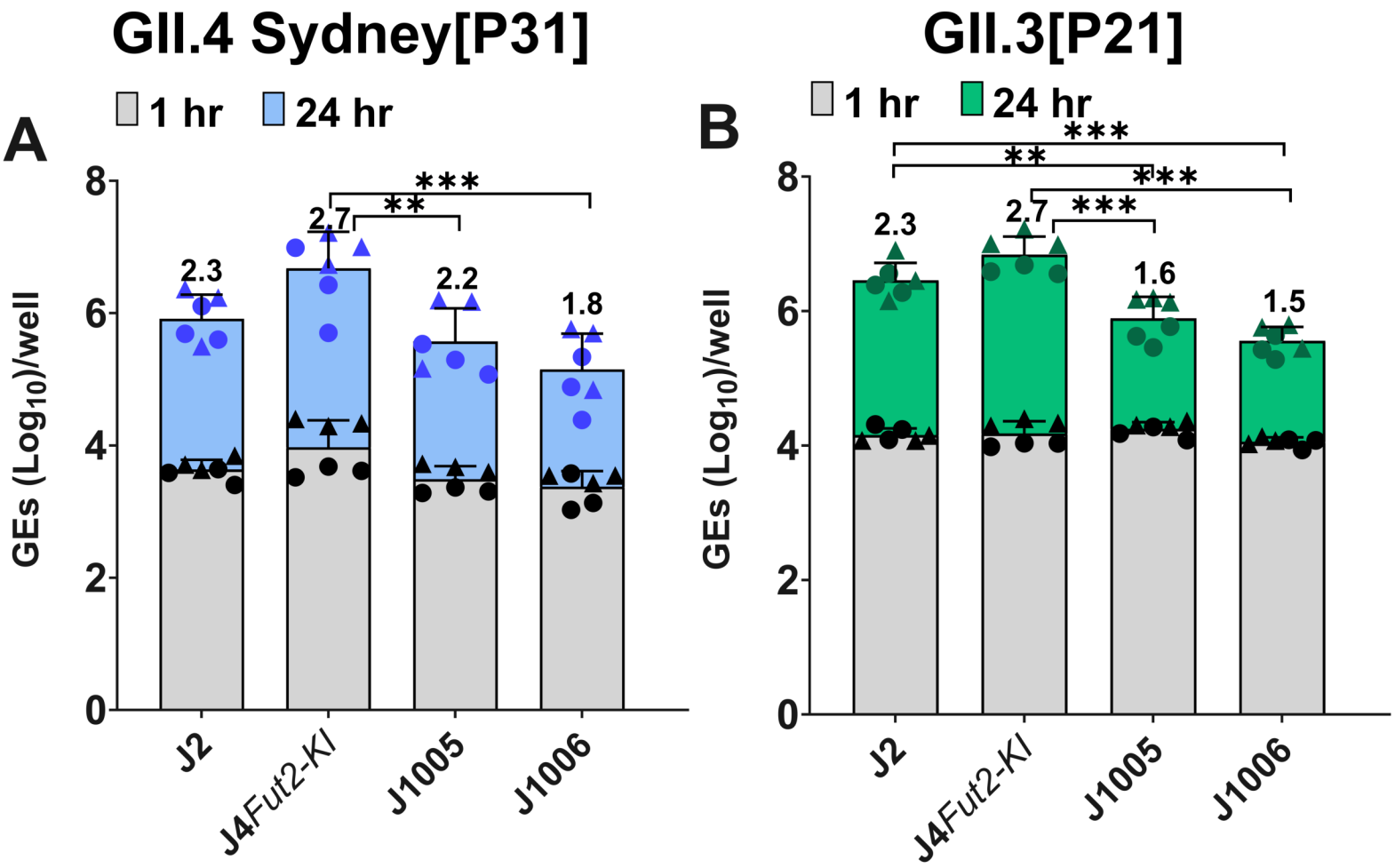
GII.4 Sydney[P31]
A
1 hr
24 hr
GEs (Log10)/well
8
6
4
2
0
2.3
2.7
2.2
1.8
***
**
J2
J4Fut2-KI
J1005
J1006
GII.3[P21]
B
1 hr
24 hr
GEs (Log10)/well
8
6
4
2
0
2.3
2.7
1.6
1.5
***
**
***
***
J2
J4Fut2-KI
J1005
J1006

	GII.4 / Sydney				GII.3			
HIEs	2002	2003	2004	2005	2002	2003	2004	2005
Duodenal	1.3 (*0.8-2.0*)	1.6 (*1.4-1.9*)	2.0 (*1.7-2.3*)	1.8 (*1.7-2.0*)	0.7 (*0.4-1.2*)	0	1.5 (*1.2-1.9*)	0.8 (*0.4-1.4*)
Jejunal	2.2 (*1.8-2.8*)	2.1 (*1.9-2.3*)	1.8 (*1.5-2.1*)	2.1 (*1.8-2.3*)	2.0 (*1.8-2.2*)	0	1.9 (*1.6-2.2*)	1.2 (*0.8-2.0*)
Ileal	2.2 (*2.0-2.5*)	2.3 (*2.1-2.4*)	1.7 (*1.4-2.0*)	2.7 (*2.5-2.8*)	1.8 (*1.2-2.6*)	0.2 (0.1-0.5)	1.3 (*1.0-1.8*)	0.6 (*0.3-1.1*)
Colonic	0	0	0	0	0	0	0	0

HIE Line	Adult/Infant	Segment	$Log_{10}(GE)/TCID_{50}$ *		
			GII.4 Sydney[P31]	**GII.4 Sydney[P16]**	**GII.3[P21]**
J2	Adult	Jejunal	3.9 (*1.07*) [5]	4.3 (*1.08*) [4]	3.7 (*1.08*) [3]
J4*FUT2-KI*	Adult	Jejunal	4.3 (*1.06*) [3]	5.1 (*1.01*) [3]	3.5 (*1.01*) [3]
J1005	Infant	Jejunal	3.7 (*1.05*) [5]	3.9 (*1.05*) [4]	3.6 (*1.09*) [3]
J1006	Infant	Jejunal	3.7 (*1.06*) [5]	3.9 (*1.04*) [4]	3.6 (*1.02*) [3]

Genogroup	Genotype	Reference strain	P Type	Cultivatable strains	Log_{10} increase in viral RNA
GI	GI.1	GI.1[P1]/1968/Norwalk	P1	1	1.9
	GI.4	**PCO-1993**	P4	1	1.1
	GI.5	**PCO-1638**	P4	1	0.6
	GI.7	**PCO-475**	ND	1	0.8
GII	GII.1	TCH18-98	P16	1	1.7
	GII.2	TCH05-951	P2	1	2.1
	GII.3	TCH04-577	P21	2	3.0
		PCO-2061	P12		1.8
	GII.4 Lanzou_2002	TCH02-276	P4	1	0.8
	GII.4 Farmington	TCH04-191	P4	2	2.3
		TCH02-539	ND		0.9
	GII.4 Hunter_2004	**TCH05-797**	P4	1	1.8
	GII.4 Yerseke_2006a	TCH07-194	P4	3	2.0
		TCH02-186	P4		1.5¶
		TCH02-276	P4		0.8¶
	GII.4 Den Haag_2006b	TCH07-882	P4	6	2.2
		MDA09-01	P4		2.4
		TCH23-323	P16		2.3
		TCH08-227	P4		1.5¶
		TCH08-429	P4		1.3¶
		TCH08-430	P4		0.9¶
	GII.4 New Orleans_2009	TCH11-64	P4	2	1.7
		TCH23-25	P4		0.9
	GII.4 Sydney_2012	TCH12-580	P31	7	2.7
		TCH14-10	P31		2.0¶
		TCH15-82	P31		2.7
		TCH15-88	P31		3.0¶
		TCH15-123	P16		2.0¶
		BCM16-1	P31		2.0
		BCM16-16	P16		2.2
	GII.4 Sydney_2015	BCM16-22	P16	4	1.8¶
		TCH19-76	P16		2.3
		BTH18-10	P16		2.0
		BTH19-9	P16		0.8
	GII.6	TCH13-106	P7	4	1.3
		TCH15-167	P7		2.9
		TCH08-166	P7		1.0¶
		CVID	ND		1.3
	GII.7	TCH06-163	P8	1	0.5¶
	GII.8	TCH09-279	P7	1	0.7
	GII.12	TCH09-477	P8	1	1.1
	GII.13	TCH10-338	ND	1	0.9
	GII.14	TCH14-364	P16	1	1.5
	GII.17	TCH14-385	P38	2	2.1
		1295-44	P13		1.5

HIE line	Source age	Phenotyping results		
		Secretor Status	**ABH** Status	**Lewis** Status
J2	52 y	Se+	B	Le^b
J4$^{FUT2/KI}$	62 y	Se+	O	Le^b
LG2002 (D,J,I,C)	34 y	Se+	O	Le^b
LG2003 (D,J,I,C)	23 y	Se+	O	Le^b
LG2004 (D,J,I,C)	25 y	Se+	A	Le^b
LG2005 (D,J,I,C)	23 y	Se+	O	Le^b
H9tHIE	18 wks •	Se+	B	Le^b
J1005	10/37 wks ••	Se+	A	Le^b
J1006	12/43 wks ••	Se+	B	Le^b
D201	56 y	Se+	O	Le^b